ISSN	0021-4922
Zeitschrift	Japanese journal of applied physics / 1
Aufsatz-Autor	
Aufsatz-Titel	
Band/Heft	44/9
Jahrgang	2005
Seiten	6546-6549
Bemerkung	

Japanese Journal of Applied Physics
Vol. 44, No. 9A, 2005, pp. 6546–6549

Ultrafast Single-Shot Optical Oscilloscope based on Time-to-Space Conversion due to Temporal and Spatial Walk-Off Effects in Nonlinear Mixing Crystal

Yoshihiro TAKAGI*, Yoshifumi YAMADA, Kiyoshi ISHIKAWA, Seiji SHIMIZU[1] and Shuji SAKABE[1]

Department of Material Science, The Graduate School of Material Science, University of Hyogo, Kamigouri-cho, Hyogo 678-1297, Japan
[1]*Advanced Research Center for Beam Science, Institute for Chemical Research, Kyoto University, Gokasyo, Uji, Kyoto 611-0011, Japan*

(Received April 26, 2005; accepted June 12, 2005; published September 8, 2005)

A simple method for single-shot sub-picosecond optical pulse diagnostics has been demonstrated by imaging the time evolution of the optical mixing onto the beam cross section of the sum-frequency wave when the interrogating pulse passes over the tested pulse in the mixing crystal as a result of the combined effect of group-velocity difference and walk-off beam propagation. A high linearity of the time-to-space projection is deduced from the process solely dependent upon the spatial uniformity of the refractive indices. A snap profile of the accidental coincidence between asynchronous pulses from separate mode-locked lasers has been detected, which demonstrates the single-shot ability. [DOI: 10.1143/JJAP.44.6546]

KEYWORDS: three-wave mixing, time-to-space conversion, pulse correlation, femtosecond, single shot, walk-off, phase matching

1. Introduction

Imaging of the time profile of the optical transients is in increasing demand in a variety of ultrafast single-shot optical measurements. Among the various nonlinear techniques reported so far the most popular ones are the frequency up-conversion (doubling or the sum-frequency generation)[1] and the Kerr optical gating,[2] which have a small-angle crossed-beam geometry that maps the time delay onto a line across the nonlinear medium. Also, self-diffraction between the interacting beams has been used as a nonlinear effect.[3] To avoid limitation of the phase-matching bandwidth and the pulse deformation due to the group-velocity dispersion, these techniques are restricted to the use of thin nonlinear media at the expense of interaction length. In order to use a semiconductor detector for a nonlinear device, a single-shot autocorrelator based on the photo-induced reflectivity change in Si was applied to testing weak infrared optical pulses.[4] Also, a nonlinear response in photocurrent from a conventional Si charge-coupled-device (CCD) array provided a direct signal acquisition for correlation profiles.[5] These techniques are free from the problems of phase matching and have a wide spectral coverage, but the time resolution is restricted more or less to picoseconds due to the carrier recombination time. Also, the signal is not background free. In all of the above-mentioned techniques that are under the single-shot regime, the incident light waves are prepared so that they have a distributed wavefront in order to convert the delay-time distribution onto the spatial dimension. The time-to-wavelength projection[6] is another type of single-shot diagnostics that uses the up-conversion with a chirped reference pulse. A technique was reported that is capable of providing both amplitude and phase information imaging of femtosecond pulses using a grating pair pulse-shaping device: it is based on spectrally decomposed three-wave mixing in nonlinear crystals.[7] However, the mixing of the spectrally resolved components required high detection sensitivity and single-shot measurement was not carried out. In addition to the concept of time-to-space projection, we should refer in this context to the development of a single-shot all-optical sampling oscilloscope using a nonlinear fiber loop mirror fitted with a retarding pulse replicator.[8] This system gives picosecond resolution but is likely to be available only in a limited wavelength range for optical fiber communication.

With a thick nonlinear mixing crystal we have developed a simple time-to-space projection (TISP) technique in autocorrelation and cross-correlation measurements using the combined effects of the group-velocity difference (GVD) of the collinearly injected pulses and the beam propagation under walk-off in a birefringent crystal. No arrangements for preparation of the distributed wavefront or spectral manipulation are required. The interval between the interacting pulses is swept by the GVD during the propagation, resulting in initiation and termination of the interaction, and the intensity correlation is printed on the generated beam that walks off away from the interacting beams. Accordingly, the interaction length is self-limited to the interval determined by the GVD irrespective of the crystal thickness (if the thickness is larger than the interaction length). Walk-off beam propagation[9] in birefringent crystals has so far been considered mostly to be a drawback because it limits the conversion efficiency in optical mixing. Here we make use of a large walk-off effect. We examined different optical mixings with the type-I and type-II phase matching and obtained a high time-to-space linearity. As a demonstration of single-shot ability, a pulse coincidence between separate mode-locked lasers has been detected. Simplicity in a TISP process that has a good linearity is advantageous to the development of a single-shot ultrafast optical oscilloscope.

2. Principle of Time-to-Space Conversion

The second-order intensity correlation at a propagation depth z between the interacting gaussian pulses with peak intensities I_1 and I_2, halfwidth $\sqrt{2\ln 2}a$, group velocities v_1 and v_2, and relative delay time τ is given as

$$G(\tau,z)=\int_{-\infty}^{\infty} I_1(t,z)\times I_2(t-\tau,z)\,dt = a\sqrt{\pi/2}I_1I_2\exp\left\{-\frac{1}{2a^2}\left[\tau-\left(\frac{1}{v_1}-\frac{1}{v_2}\right)z\right]^2\right\}. \quad (1)$$

When $v_1 \neq v_2$, a profile of $G(\tau,z)$ in terms of z with a given τ represents a spatially developed replica of cross correlation

*Corresponding author.

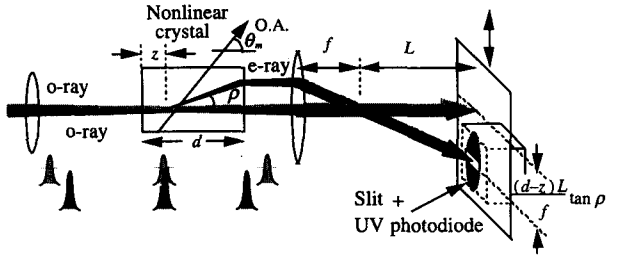

Fig. 1. Arrangement for time-to-space projection using type-I (oo → e) sum-frequency generation. The slit and UV photodiode with the translation stage would not be necessary if they could be replaced by a UV diode array.

Table I. Parameters of time-to-space projection for BBO with the fundamental wavelength of 0.78 μm.

Nonlinear process	θ_m	v_1, v_2 (μm/ps)	$1/v_1 - 1/v_2$ (fs/mm)	$\rho(\theta_m)$
Type-I THG	45.7°	168, 178	330	4.89°
Type-II SHG	42.5°	178, 184	201	4.39°
Type-II THG	57.3°	168, 188	642	4.30°

θ_m: phase-matching angle, $1/v_1 - 1/v_2$: difference of propagation time, $\rho(\theta_m)$: walk-off angle at phase matching. THG is the sum-frequency generation from the fundamental and its second harmonic. For SHG, v_1 and v_2 are the group velocities of the ordinary (o) ray and extraordinary (e) ray, respectively. For THG, v_1 and v_2 are the group velocities of the second harmonic and the fundamental, respectively. Refractive indices for BBO used in the calculation were taken from ref. 9.

that is measured usually as a function of τ under the condition $(1/v_1 - 1/v_2)d \ll a$, where d is the length of the nonlinear crystal. The principle of TISP is depicted in Fig. 1. The time difference τ between the pulses injected along a collinear line is adjusted so that the pulses overlap at a position z in the crystal according to GVD. The crystal is aligned for the best phase matching. The sum-frequency beam propagating in the direction of the walk-off angle ρ converts the time-integrated intensity at z to its beam cross section, giving rise to a projection of the interaction profile into the beam profile. The difference in propagation time $1/v_1 - 1/v_2$ thus represents the measurable duration time of the input lights per unit propagation length. Related parameters for the β-barium borate (BBO) crystal are listed in Table I.

3. Experiments and Results

The experiment of the TISP for the type-I sum-frequency mixing (i.e., third-harmonic generation, THG) was performed using a BBO crystal with a length of $d = 8$ mm cut at $\theta = 35°$. The incident lights are the fundamental and its second harmonic (SH) from a regeneratively amplified self-mode-locked Ti:sapphire laser (Coherent, MiRA/ReGA) oscillating at 0.78 μm and with a repetition rate of 100 kHz and a pulse energy of 0.5 μJ. The incident beams, polarized perpendicular (o-rays) to the optic axis, were focused onto the crystal with a lens of focal length $f = 120$ mm. The output sum-frequency beam (e-ray) passed a 19-mm-focal-length lens placed ~15 mm behind the exit of the crystal so that the beam is collimated and the separation from the incident beams is magnified properly. The intensity profile

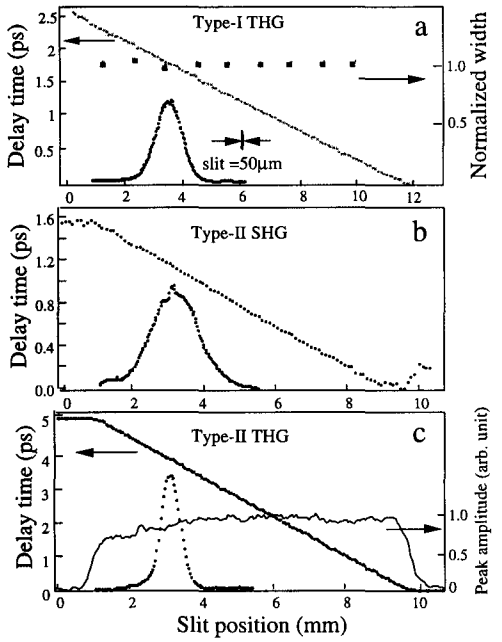

Fig. 2. Relationship of position of spot to time difference of incident pulses. (a) type-I THG together with the relative spot width (normalized to the profile corresponding to the temporal width of 260 fs), (b) type-II SHG, and (c) type-II THG together with the position dependence of the peak amplitude. Typical spot profiles are shown in all panels.

of the spot was measured by sliding a 50-μm-wide slit mounted on a UV photodiode along the beam cross section. Taking into account the maximum stroke (13 mm) of the sliding stage, the photodiode was positioned ~360 mm behind the collimating lens. The relationship of the position of the profile peak and the relative delay time τ is shown in Fig. 2(a) together with a typical spot profile and the position dependence of the spot width. The largest τ of 2.6 ps coincides with the attainable delay time $(1/v_1 - 1/v_2)d \approx$ 2.6 ps. The 12-mm-range of the slit position leads to a beam separation of 0.67 mm at the exit of the crystal, in accordance with the walk-off separation $d \tan \rho(\theta_m) =$ 0.68 mm. Satisfactory linearity in the dependence of the delay time on the slit position over the entire range is deduced from the fact that the process is dependent solely on the spatial uniformity of the refractive indices responsible for the group velocity and the beam walk-off and is not sensitive to geometrical conditions as in the crossed-beam arrangement. The width of the spot was nearly independent of the depth at which the sum-frequency was generated, and this is consistent with the very small pulse broadening by the second-order dispersion of the refractive index[10] for pulse durations >100 fs and a propagation length of 8 mm.

The finite size of the interacting beams limits the time resolution of the TISP profile. If Gaussian beams with a width w are assumed, the spot width w_s of the sum-frequency beam at the exit of the crystal is given as a convolution,

$$w_s = \sqrt{\tau_G{}^2 v_1{}^2 v_2{}^2 \tan^2 \rho(\theta_m)/(v_1 - v_2)^2 + w^2/2}, \quad (2)$$

where τ_G is the correlation width. Substituting into eq. (2) $w_s = 66$ μm, which is estimated from the spot width of

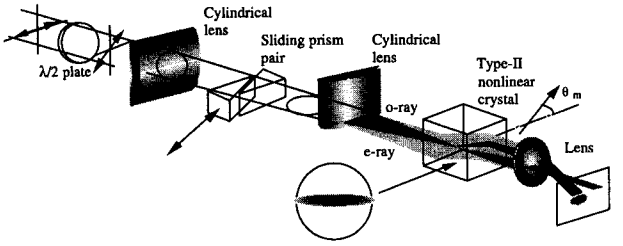

Fig. 3. Optical setup of in-line time-to-space converter for type-II (eo → e) phase matching. The beam pattern in the interaction area is shown in the inset.

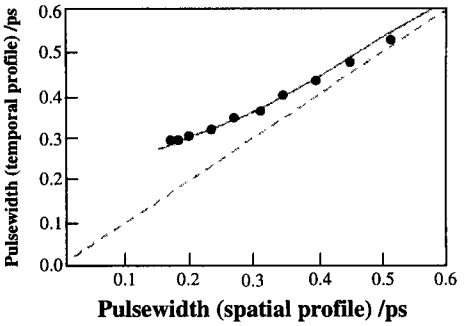

Fig. 4. Comparison of pulse widths measured by TISP and a delay-time-scan autocorrelator for light source with different pulse widths. The solid curve shows an integration of eq. (1) with respect to z for $d = 2$ mm. The broken line is a guide for the coincidence between the two methods.

1.2 mm and the magnification factor of 18, and $w = 50\,\mu$m in our experimental conditions, we obtain $\tau_G = 220$ fs. Comparing this with the temporal width of 260 fs determined by the slope of the TISP profile in Fig. 2(a), we infer that the observed spatial profile (calculated in terms of the time profile) is roughly 15% larger than the value of τ_G resulting from the "beam-size" influence.

For application of the TISP to the pulse diagnostics of the fundamental, the type-II autocorrelation measurement has been carried out with a compact in-line arrangement, as shown in Fig. 3, keeping in mind the ease of handling for daily operation. The nonlinear medium is an 8-mm-thick type-II BBO crystal cut at $\theta = 41°$. The polarization of the input beam is tilted by 45° with a half-wave plate so that the beam contains both o- and e-rays for creating GVD. After the beam passes through a cylindrical lens ($f = 300$ mm) the upper half of the beam goes through the second cylindrical lens ($f = 100$ mm) resulting in the formation of an overlapped point-and-line-focused pattern in the crystal, along the plane containing the optic axis (shown in the inset of Fig. 3). By choosing the initial beam size properly, the overlap of the point and line spots is maintained throughout the crystal so that the interaction can take place at any depth under the beam walk-off for the e-ray. For compensation of the delay caused by the second cylindrical lens in the upper half of the beam, a pair of 30° prisms, one of them movable, are inserted across the lower half of the beam between the cylindrical lenses. A blue filter was inserted in front of the photodiode (not shown in Fig. 3) because one of the transmitted beams (the expanded one) covers the sum-frequency beam. Linearity in the dependence of the delay-time on the slit position is very good, as shown in Fig. 2(b). Also shown is a typical spot profile taken by a photodiode array. The delay-time range of 1.5 ps coincides with the expected GVD in Table I.

The TISP performance in terms of time resolution was compared with the conventional autocorrelation (driven by the delay-time scan) using a 2-mm-length type-II BBO for different pulse widths of the light source. In Fig. 4 the abscissa shows the pulse width obtained by the TISP profile (without correction for the influence by the finite beam size), and the ordinate is the pulse width taken by the conventional autocorrelator. Gaussian pulses were assumed. The pulse widths taken by the latter method present a departure from those by the former in the region ≤ 0.4 ps. This is because the latter method measures the integration of eq. (1) with respect to z over the crystal length (2 mm) for $1/v_1 - 1/v_2 = 201$ fs/mm, while the former method registers the correlation profile on the sum-wave beam cross section as a function of z for a fixed τ. The pulse width is calculated without consideration of the beam-size effect. Reasonable fit with the experiment proves that the beam-size effect is dramatically reduced (< 1% for the pulse of $\tau_G = 250$ fs) compared with the type-I THG because of the lower GVD, and that the type-II TISP suits the autocorrelation measurement in the present time scale.

A type-II THG has been measured using the same arrangement as that shown in Fig. 3 except for replacing the half-wave plate by a doubling crystal (BBO, type-I). Then, the collinear fundamental (e-ray) and SH (o-ray) beams with orthogonal polarizations were injected in the mixing crystal under the type-II interaction. An excellent linearity between the relative delay time and the peak position of the TISP profile was confirmed, as shown in Fig. 2(c) (shown together with a spot profile and the position dependence of the peak amplitude). The delay-time range of 5.0 ps agrees with the GVD parameter in Table I. The highest accessible time span was obtained with the highest GVD among the three kinds of optical mixings, while the profile suffers from considerable beam-size influence with the broadening by 45% for the pulse of $\tau_G = 240$ fs. The shortest interaction length obtained was 0.37 mm from the values of τ_G and GVD in Table I. From the fact that such a short interaction length is enough for a sufficient signal intensity it should be noted that the pulse width down to $\tau_G = 74$ fs is available if the TISP autocorrelation with type-II SHG is applied (GVD = 201 fs/mm), although the present work is limited by the pulse width of the light source. The roughness in the peak amplitude along the slit position is attributed to scratches and blur on the rear surface of the crystal. For application to further short-pulse measurements, the interaction length must be considered in terms of the phase-matching bandwidth[9] and the second-order dispersion of the refractive index, as well as the selection of nonlinear medium with a large birefringence (such as the organic nonlinear crystals) for resolvable spatial projection.

As a demonstration of the single-shot ability of TISP, a pulse-timing map between separate mode-locked lasers was detected. The light sources are the fundamental at 0.78 μm described above and a separate self-mode-locked Ti:sapphire laser oscillating at 0.82 μm and with a pulse rate of 76 MHz and a pulse energy of 0.5 nJ. They have orthogonal polar-

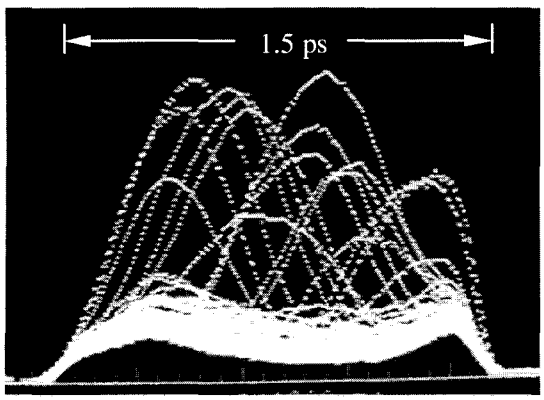

Fig. 5. TISP profiles of pulse coincidence in a time interval of 1.5 ps between separate mode-locked lasers with 100 kHz and 76 MHz pulse repetition rates. Exposure time is 2 s.

izations. The TISP profile of sum-frequency mixing was observed, as shown in Fig. 5, using the type-II BBO crystal above and a UV image scope. The measurable time span is estimated to be 1.5 ps. Since there is no synchronism between the pulses, the average rate of pulse coincidence within this time interval is $1.5\,\text{ps} \times 76\,\text{MHz} \times 100\,\text{kHz} = 11\,\text{s}^{-1}$. The TISP profile gives a consistent result with respect to the rate and irregularity of the pulse coincidence. It is noted that the single-shot optical mixing was carried out using a pair of input pulses with typical energies of 0.5 μJ and 0.5 nJ. The detectability limit is expected to be at least one order of magnitude lower in range for either one of the input energies.

In the present work, the temporal information was dispersed on the plane containing the optic axis of the nonlinear crystal. The other axis is preserved for the simultaneous acquisition of different pieces of information, such as spectral structure.

4. Summary

We have demonstrated a simple single-shot correlation technique based on the self-acting highly linear time-to-space projection due to the temporal and spatial walk-off beam propagation in the three-wave mixing process. This method was found to be readily applicable to autocorrelation (type-II) and cross correlation (type-I and type-II) for single-shot pulse diagnostics. The use of a thick nonlinear crystal allowed a measurable time span of 5 ps, while the interaction-length-limited mixing maintains a time resolution of 180 fs (defined by the pulse width that has 1% broadening due to the beam-size influence). Construction of a single-shot sub-picosecond optical oscilloscope and development of the up-conversion spectroscopy[11] needed for short-lived single-shot fluorescence studies are useful applications of the present technique.

Acknowledgement

We gratefully acknowledge the loan of a UV scope by Hamamatsu Photonics K.K. We thank F. Sato and S. Okihara at Osaka university for assistance with the laser operation.

1) F. Salin, P. Georges, G. Roger and A. Brun: Appl. Opt. **26** (1987) 4528.
2) B. S. Prade, J. K. Schins, E. T. J. Nibbering, M. A. Franco and A. Mysyrowicz: Opt. Commun. **113** (1994) 79.
3) T. S. Clement, A. J. Taylor and D. J. Kane: Opt. Lett. **20** (1995) 70.
4) L. Zheng and D. D. Meyerhofer: Opt. Lett. **20** (1995) 407.
5) Y. Takagi, T. Kobayashi, K. Yoshihara and S. Imamura: Opt. Lett. **17** (1992) 658.
6) T. Miura, K. Kobayashi, K. Takasago, Z. Zhang, K. Torizuka and F. Kannari: Opt. Lett. **25** (2000) 1795.
7) P. C. Sun, Y. T. Mazurenko and Y. Fainman: J. Opt. Soc. Am. A **14** (1997) 1159.
8) K. L. Deng, R. J. Runser, I. Glesk and P. R. Prucnal: IEEE Photonics Technol. Lett. **10** (1998) 397.
9) V. G. Dmitriev, G. G. Gurzadyan and D. N. Nikogosyan: *Handbook of Nonlinear Optical Crystals* (Springer, New York, 1999) 3rd ed.
10) Siegman: *Lasers* (University Science Books, Mill Valley, CA, 1986) p. 332.
11) T. Kobayashi, Y. Takagi, H. Kandori, K. Kemnitz and K. Yoshihara: Chem. Phys. Lett. **180** (1991) 416.